# A Vertically Averaged Circulation Model Using Boundary-Fitted Coordinates

MALCOLM L. SPAULDING[1]

*Continental Shelf Institute, Håkon Magnussonsgt. 1B, 7000 Trondheim, Norway*

(Manuscript received 27 July 1983, in final form 12 March 1984)

ABSTRACT

A two-dimensional vertically averaged circulation model using boundary-fitted coordinates has been developed for predicting sea level and currents in estuarine and shelf waters. The basic idea of the approach is to use a set of coupled quasi-linear elliptic transformation equations to map the physical domain to a corresponding transformed plane such that all boundaries are coincident with coordinate lines and the transformed mesh is rectangular. The hydrodynamic equations are then solved by a multi-operation finite difference technique in the rectangular mesh transformed grid. Comparisons of the circulation model predictions for tidally forced flows in a wedge section with both flat and quadratic bottom topography, and in a flat channel with exponential variation in width, were in excellent agreement with corresponding analytic solutions. Simulation of steady-state wind-induced setup in a closed basin formed using elliptic cylindrical coordinates also was in excellent agreement with the analytic solution. Finally, the model was applied to predict the $M_2$ tidal circulation in the North Sea and accurately reproduced the well-known amphidromic systems present in this region.

## 1. Introduction

The last two decades have seen extensive development and application of hydrodynamic models for predicting circulation in coastal and shelf waters (Gordon and Spaulding, 1974; Hinwood and Wallis, 1975; ASCE, 1980), with the majority of these studies employing well known finite difference techniques on a rectangular grid. While this approach has proven extremely useful in various applications, there are many times when the computational costs for achieving a useful prediction become excessive. This situation typically arises when it is necessary to include large variations in spatial scale within the study region in order to represent features such as coastal boundary-layer dynamics, flows in channels, embayments and around islands, and flows near engineered structures (offshore discharge/intake, towers, dredged channels, disposal mounds, etc.). If the grid spacing is made small enough to resolve the smallest spatial scales of interest such that accurate predictions can be made, the computational costs often become excessive. On the other hand, if the number of mesh points is not large enough the numerical predictions may be grossly in error throughout the solution domain.

Because of the importance of this issue, numerous investigators have attempted to use alternative solution methodologies to allow increased user control of grid placement. Examples include the following: finite element techniques (with the triangular mesh being the most popular) (Pinder and Gray, 1977), and finite difference methods using conformal curvilinear grids (Reid *et al.*, 1977; Wanstrath, 1977); orthogonal curvilinear grids (Waldrop and Tatom, 1976; Blumberg and Herring, 1982); stretched rectangular grids (Waldrop and Farmer, 1974; Peffley and O'Brien, 1976; Butler, 1980); irregular (triangular) grids (Thacker, 1977) and boundary-fitted coordinates (Johnson, 1980, 1982).

The goal of this paper is to present a circulation model that allows extensive user flexibility in spacing of the grid structure, but at the same time retains the simplicity, elegance and well documented characteristics of the rectangular finite difference techniques. This goal is accomplished by using a set of coupled quasi-linear elliptic transformation equations to map an arbitrary multiconnected region from physical space to a rectangular mesh structure in the transformed plane. The hydrodynamic equations are then solved on the transformed mesh. In the text that follows the solution methodology, derivations of the governing equations for both mesh generation and the circulation model are presented. This is followed by a discussion of the computational approach for solving the equations, and the application of the system to some case examples with known analytic solutions. Finally, a preliminary application of the model to tidal circulation in the North Sea is outlined to illustrate the model's usefulness for practical calculations.

## 2. Generation of boundary-fitted coordinate systems

The basic idea of the proposed boundary-fitted coordinate system approach is to generate transformation

[1] Permanent address: Department of Ocean Engineering, University of Rhode Island, Kingston, RI 02881.

© 1984 American Meteorological Society

functions such that all boundaries are coincident with coordinate lines. Following the extensive work of Thompson *et al.* (1974, 1976, 1977a,b) and Thames *et al.* (1975, 1977), the natural coordinates $\xi$ and $\eta$ are taken as solutions of an elliptic boundary value problem with one of the coordinates constant on the boundaries.

The curvilinear coordinates are determined by solving an elliptic system of the form

$$\xi_{xx} + \xi_{yy} = P(\xi, \eta), \tag{1a}$$

$$\eta_{xx} + \eta_{yy} = Q(\xi, \eta), \tag{1b}$$

with Dirichlet boundary conditions, the $\xi$ coordinate being specified as constant on one boundary and equal to another constant on the opposite boundary. The $\eta$ coordinate then varies monotonically over the same range on both the boundaries. Subscripts indicate differentiation and will be used in the text to follow.

Since we desire to perform all numerical computations in a uniform rectangular transformed plane, the dependent and independent variables in Eq. (1) must be interchanged. This results in a coupled system of quasi-linear elliptic equations for determining $x(\xi, \eta)$ and $y(\xi, \eta)$ in the transformed plane, and is given by

$$\alpha x_{\xi\xi} - 2\beta x_{\xi\eta} + \gamma x_{\eta\eta} = -J^2[x_\xi P(\xi, \eta) + x_\eta Q(\xi, \eta)], \tag{2a}$$

$$\alpha y_{\eta\eta} - 2\beta y_{\xi\eta} + \gamma y_{\eta\eta} = -J^2[y_\xi P(\xi, \eta) + y_\eta Q(\xi, \eta)], \tag{2b}$$

where

$$\left.\begin{aligned} \alpha &= x_\eta^2 + y_\eta^2, & \gamma &= x_\xi^2 + y_\xi^2 \\ \beta &= x_\xi x_\eta + y_\xi y_\eta, & J &= x_\xi y_\eta - x_\eta y_\xi \end{aligned}\right\}. \tag{2c}$$

While this set of equations is considerably more complex than the original set, the boundary conditions are now specified on straight lines and the coordinate spacing is uniform in the transformed plane. It should further be noted that the orthogonal and conformal curvilinear grids, as well as the simple stretched rectangular grids, are special cases of the boundary-fitted coordinate approach given here.

The functions $P(\xi, \eta)$ and $Q(\xi, \eta)$ may be used to move the coordinate lines within the solution domain. While the choice of these functional relationships is arbitrary, Thompson *et al.* (1977a), after much computer experimentation, have selected a sum of decaying exponentials given by

$$P(\xi, \eta) = -\sum_{i=1}^{n} a_i \operatorname{sgn}(\xi - \xi_i) \exp[-c_i(\xi - \xi_i)] - \sum_{k=1}^{m} b_k \operatorname{sgn}(\xi - \xi_k) \times \exp\{-d_k[(\xi - \xi_k)^2 + (\eta - \eta_k)^2]^{1/2}\}, \tag{3a}$$

$$Q(\xi, \eta) = -\sum_{j=1}^{l} a_j \operatorname{sgn}(\eta - \eta_j) \exp[-c_j(\eta - \eta_j)] - \sum_{k=1}^{m} b_k \operatorname{sgn}(\eta - \eta_k) \times \exp\{-d_k[(\xi - \xi_k)^2 + (\eta - \eta_k)^2]^{1/2}\}, \tag{3b}$$

where the positive amplitudes and decay factors are not necessarily the same in the two equations, being particularly useful for problems in engineering fluid mechanics.

The first terms have the effect of attracting the $\xi$ = constant lines to the $\xi = \xi_i$ lines (3a), and the $\eta$ = constant lines to the $\eta = \eta_i$ lines (3b). The second terms cause $\xi$ = constant lines to be attracted to the point $(\xi_k, \eta_k)$ in Eq. (3a) and a similar effect on $\eta$ = constant lines in Eq. (3b).

The solution to the finite difference approximations of Eqs. (2a) and (2b) were obtained by point SOR iteration (Roache, 1972). All derivatives were approximated by second-order central difference operators. The actual values of the curvilinear coordinates $\xi$ and $\eta$ used to specify the boundary points are irrelevant to later use of the coordinate system since $\Delta\xi$ and $\Delta\eta$ simply cancel out of all difference expressions for transformed derivatives. The data for defining the boundaries of the study domain can therefore be obtained from any chart or map as long as the scaling parameters are known.

As a practical illustration let us consider the application of the methodology to define a grid system for the North Sea (Fig. 1a). Figure 1b shows the proposed boundaries of the body in the transformed plane, while Fig. 1c displays the results of the solution to Eq. (2) in the physical plane. The ability to control the structure of the grid system by selecting the representation in the transformed plane and the coordinates of the boundary points is clearly evident. As a further illustration of the flexibility of the method for controlling grid spacing, Fig. 1d presents the same case as above, but with point attraction, near a known amphidromic point in the southern North Sea. Note that the total number of grid cells has not changed; only their location has been modified. While Fig. 1d shows only the case of point attraction in one region, the methodology allows any number of regions of attraction and/or repulsion to either lines and/or points.

## 3. Derivation of the hydrodynamic equations in boundary-fitted coordinates

Anticipating the use of this circulation model for regions with substantial variations in latitude the two dimensional vertically averaged equations of motion and continuity in spherical coordinates have been adopted for the present investigation.

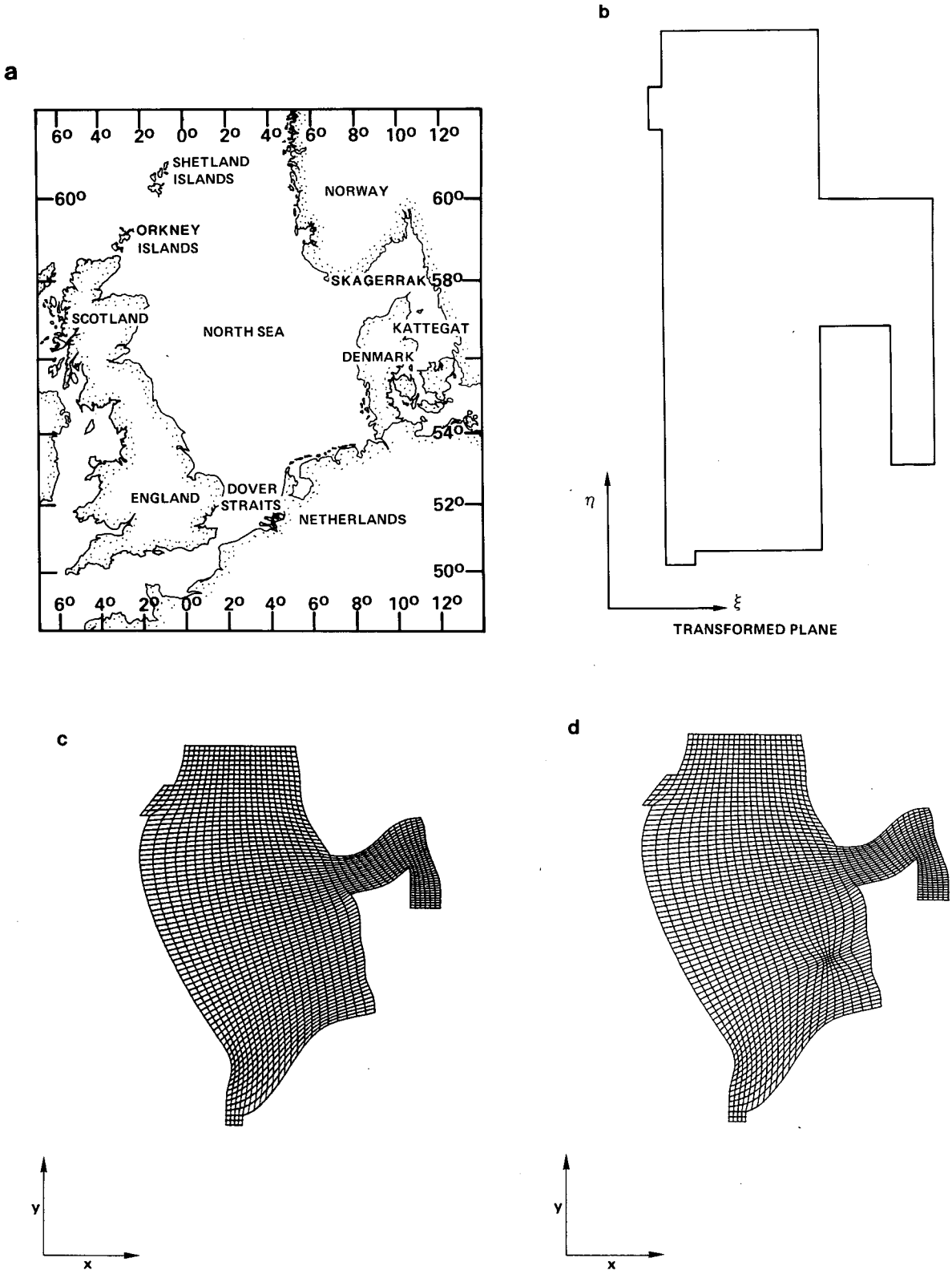


FIG. 1. Illustration of the application of the boundary-fitted coordinate system to the North Sea. (a) Study area; (b) grid system in the transformed plane; (c) grid system in the physical plane; (d) grid system in the physical plane with point coordinate attraction.

Following Mathisen and Johansen (1983), the vertically averaged equations of motion in the latitudinal ($\phi$) and longitudinal ($\kappa$) directions are given, respectively, as

$$U_t + \frac{U}{R} U_\phi + \frac{V}{R\cos\phi} U_k + \frac{V^2}{R}\tan\phi + \frac{g}{R}\zeta_\phi - 2V\omega\sin\phi - \frac{1}{R} P_{a_\phi} + \frac{\tau_{b,\phi}}{d} - \frac{\tau_{s,\phi}}{d} = 0, \quad (4)$$

$$V_t + \frac{U}{R} V_\phi + \frac{V}{R\cos\phi} V_\kappa - \frac{UV}{R}\tan\phi + \frac{g}{R\cos\phi}\zeta_\kappa + 2U\omega\sin\phi + \frac{1}{R\cos\phi} P_{a_\kappa} + \frac{\tau_{b,\kappa}}{d} - \frac{\tau_{s,\kappa}}{d} = 0, \quad (5)$$

where $U$ and $V$ are the vertically averaged velocities, $d$ is the total depth, $R$ the mean radius of the earth, $\omega$ the angular speed of the earth's rotation, $P_a$ atmosphere pressure, $\zeta$ the sea-surface elevation, and $\tau_s$ and $\tau_b$ the surface and bottom stress vectors.

The bottom stress vector is expressed as

$$\tau_{b_{\phi,\kappa}} = \frac{\rho g(U, V)(U^2 + V^2)^{1/2}}{C^2}, \quad (6a)$$

where $C$ is the Chezy coefficient, $\rho$ the sea water density and $g$ is gravitational acceleration. The surface stress is similarly given in quadratic form as

$$\tau_{s_{\phi,\kappa}} = \rho_a C_D(W_\phi, W_\kappa)(W_\phi^2 + W_\kappa^2)^{1/2}, \quad (6b)$$

where $W$ denotes wind speed, $\rho_a$ the density of air and $C_D$ the drag coefficient.

To complete the set of equations, the vertically integrated equation of water mass conservation is given by

$$\zeta_t + \frac{1}{R}(Ud)_\phi + \frac{1}{R\cos\phi}(Vd)_\kappa - \frac{dU}{R}\tan\phi = 0. \quad (7)$$

Equations (4), (5) and (7) with the auxiliary relationships given by Eqs. (6a) and (6b) define the governing equations. On the closed boundaries the normal velocities are set to zero:

$$V_n(s, t) = 0, \quad (8)$$

where $V_n$ is the normal component of velocity at position $s$. At open boundaries either the vertically averaged velocity or sea-surface elevation are specified as a function of time.

Since it is desired to perform all computations in the transformed plane, where the mesh system consists of simple rectangles, Eqs. (4), (5) and (7) must be transformed such that $\xi$ and $\eta$ are the independent variables.

Using the fully conservative form of the differential operators given by

$$f_x = \frac{1}{J}[(fy_\eta)_\xi - (fy_\xi)_\eta], \quad (9a)$$

$$f_y = \frac{1}{J}[-(fx_\eta)_\xi + (fx_\xi)_\eta], \quad (9b)$$

where $f$ denotes some arbitrary function and $J$ is the Jacobian defined in Eq. (2c), the governing equations become

$$U_t + \frac{U}{RJ}[(Uy_\eta)_\xi - (Uy_\xi)_\eta] + \frac{V}{(R\cos\phi)J}[-(Ux_\eta)_\xi + (Ux_\xi)_\eta] + \frac{V^2}{R}\tan\phi + \frac{g}{RJ}[(\zeta y_\eta)_\xi - (\zeta y_\xi)_\eta] - 2V\omega\sin\phi - \frac{1}{RJ}[(P_a y_\xi)_\xi - (P_a y_\xi)_\eta] + \frac{\tau_{b,\phi}}{d} - \frac{\tau_{s,\phi}}{d} = 0, \quad (10)$$

$$V_t + \frac{U}{RJ}[(Vy_\eta)_\xi - (Vy_\xi)_\eta] + \frac{V}{(R\cos\phi)J}[-(Vx_\eta)_\xi + (Vx_\xi)_\eta] + \frac{g}{(R\cos\phi)J} \times [-(\zeta x_\eta)_\xi + (\zeta x_\xi)_\eta] + 2U\omega\sin\phi + \frac{1}{(R\cos\phi)J} \times [-(P_a x_\eta)_\xi + (P_a x_\xi)_\eta] + \frac{\tau_{b,\kappa}}{d} - \frac{\tau_{s,\kappa}}{d} = 0, \quad (11)$$

$$\zeta_t + \frac{1}{RJ}[(y_\eta Ud)_\xi - (y_\xi Ud)_\eta] + \frac{1}{(R\cos\phi)J} \times [-(x_\eta Vd)_\xi + (x_\xi Vd)_\eta] - \frac{dU}{R}\tan\phi = 0. \quad (12)$$

Note that the addition of the horizontal dispersive terms could readily be achieved even though the transformation step is relatively cumbersome.

Transforming the boundary conditions, the no normal flux condition at closed boundaries is expressed as

$$\left.\begin{aligned} Vx_\xi &= Uy_\xi \text{ along lines of constant } \eta \\ Vx_\eta &= Uy_\eta \text{ along lines of constant } \xi \end{aligned}\right\}. \quad (13)$$

In addition, the surface elevation gradient normal to the closed boundary also must be specified such that the conditions of Eq. (13) are met. The open boundary conditions remain the same as previously described, with either surface elevation or velocity prescribed as a function of time.

## 4. Computational procedure

The first step in the computational procedure is to solve the transformation equations (2) given a definition of the domain in terms of the $x$ and $y$ coordinates of boundary points along lines of constant $\xi$ and $\eta$. Once convergence of the SOR point iteration is achieved (with convergence errors on the order of $10^{-4}$),

defining the $x$, $y$ locations along lines of constant $\xi$ and $\eta$, the spatial derivatives $x_\eta$, $y_\eta$, $x_\xi$ and $y_\xi$, and Jacobian $J$ at each grid point are computed using second-order central differences for interior points and backward second-order differences along the boundaries. These derivatives, scaled to the appropriate size, are then available as input to the circulation model and constitute a complete description of the mesh geometry.

Given this definition of the mesh system, the equations of motion (10) and (11) and the continuity equation (12) are solved using the multi-operational method of Leendertse (1967) on a space-staggered grid system (Method C grid of Arakawa and Lamb, 1977). This solution technique consists of two operations advancing the solution first from time level $n$ to $n + \frac{1}{2}$ and finally to $n + 1$. In the first step, $U$ and $\zeta$ are advanced from $n$ to $n + \frac{1}{2}$ by an implicit calculation in the $\phi$ direction while an explicit calculation of $V$ is completed in the $\kappa$ direction. During the second step an implicit calculation for $V$ and $\zeta$ in the $\kappa$ direction is made, followed by an explicit sweep in the $\phi$ direction for $U$, advancing the solution from $n + \frac{1}{2}$ to $n + 1$. Subsequent steps simply repeat the calculation sequence to advance the solution in time. The interested reader is referred to Leendertse (1967) for a more detailed presentation of the method or to Mathisen (1980) for its implementation in spherical coordinates.

To assure geometrically consistent and accurate mapping from the physical to the transformed plane, the transformation derivatives $x_\eta$, $y_\eta$, $x_\xi$ and $y_\xi$, and the resulting Jacobian were defined at all variable locations of the hydrodynamic model grid. This requires that the grid transformation calculations be performed on a grid with twice the resolution of the circulation model.

The use of this higher resolution grid for the transformation calculations removes the need for averaging the transformation derivatives in the circulation model and assures a geometrically conservative mapping.

## 5. Model applications

### *a. Test cases*

Model formulation and implementation, in computer code, were tested using a series of illustrative case examples in which analytic solutions were available for comparison and determination of model performance.

In all test cases the nonlinear convective acceleration terms were removed and the governing equations solved on a Cartesian coordinate system.

Consider the case of a tidal wave entering a frictionless channel of constant depth with exponential variation of width. At the channel walls the normal flow was set to zero and at either end of the channel the surface elevation was specified using the analytic solution (Ippen, 1966). Coriolis forces were assumed to be zero. The coordinate geometry was computed using the boundary-fitted coordinate generation procedure with the coordinates of the channel walls and ends used as input. Figure 2 shows a comparison between the computed and analytic model results for sea-surface elevation versus distance along the channel at $\frac{1}{12}$ increments of the forcing function period. The agreement is excellent throughout the entire simulation.

As an additional test of the model the propagation of waves into a wedged-shaped domain, as suggested by Lynch and Gray (1978), was performed. The grid configuration shown in Fig. 3 was used to describe the study area. At the walls, $r = r_0$, $\theta = 0$ and $\theta = 45°$, no flow was allowed while the free surface elevation was prescribed to vary sinusoidally with uniform amplitude and phase along $r = r_1$. Neglecting bottom friction and Coriolis forces the model was run until steady state conditions were achieved. Figures 4 and 5 show the surface elevation and velocity for the flat bottom and quadratic sloping bottom cases, respectively. In each case the agreement between analytic and model solutions is excellent. The radial symmetry exhibited by the analytic solution is also accurately reproduced by the model results.

To test the model on a somewhat more unusual geometry where significant variations in plan form and grid spacing occur, while at the same time maintaining symmetry, consider the closed basin shown in Fig. 6. The boundary conditions for the grid generation step were specified using an elliptic cylindrical coordinate system (Rottman, 1960). For the test cases shown here, the basin was assumed to be 90 km in length, 17 km in width at its narrowest point (66 km at its widest), with a constant basin depth of 10 m. The grid spatial resolution varied from 1.4 to 12 km with all grids having a constant aspect ratio of 1.85.

Following the prototype test case of Blumberg and Herring (1982) for the steady state response to wind forcing in this complex basin, the model was started from rest and driven by a constant wind stress of 1 dyne $cm^{-2}$. The bottom friction factor, specified using a quadratic formulation, was maintained constant with a Chezy coefficient of 10. Cases studied included northerly- and easterly-directed wind stresses.

After steady state conditions were achieved ~40 h after the start of the simulation, the predicted sea-surface slopes were in excellent agreement with the simple analytic solution of Horikawa (1978). The required symmetry of the wind-induced setup is clearly evident in the model-predicted values (Figs. 7a and b), even given this complex geometry.

### *b. North Sea simulations*

To provide an additional test of the proposed circulation model, application was made to predict the $M_2$ vertically averaged tidal circulation in the North

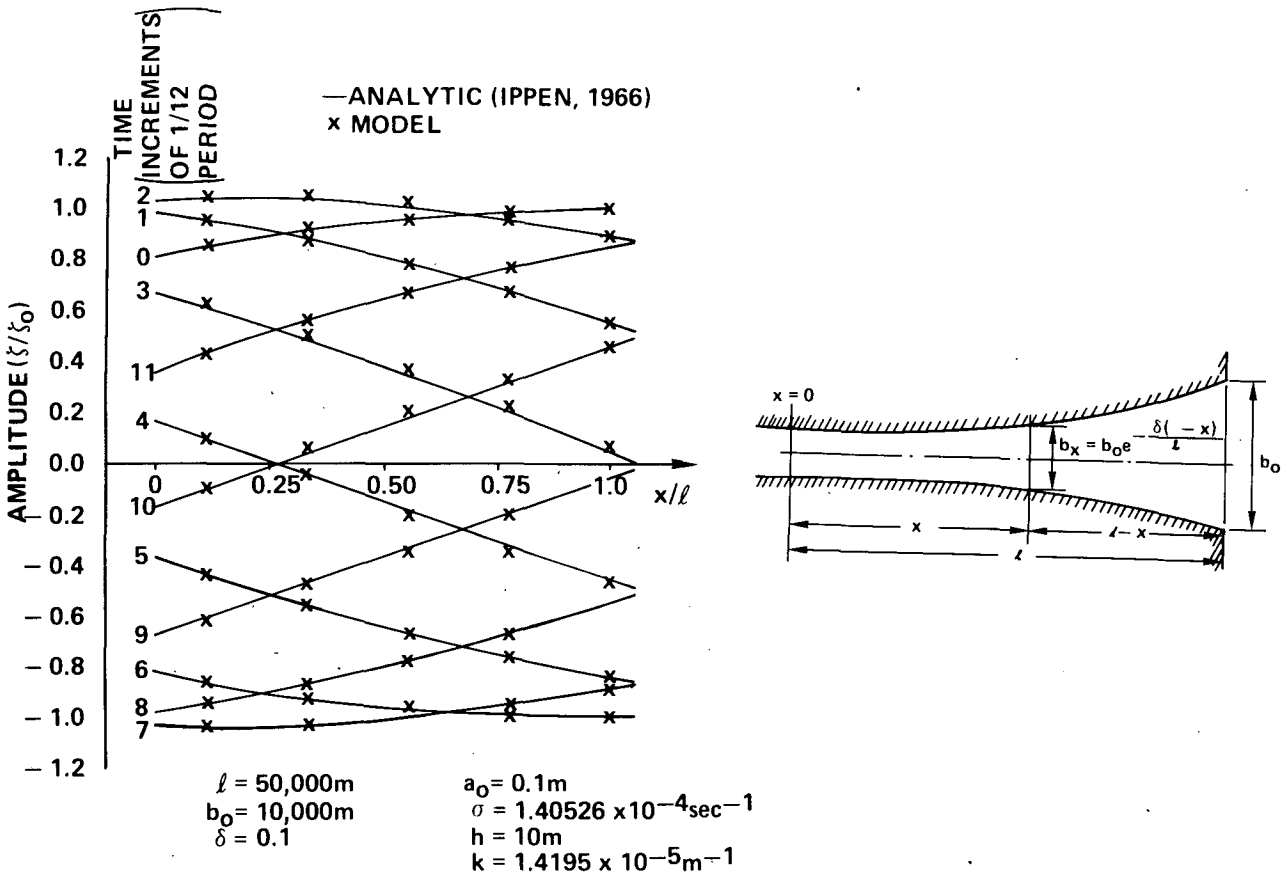


FIG. 2. Comparison of circulation model predictions with the analytic solution for sea-surface elevation versus distance along the channel, at $^1/_{12}$ increments of the forcing period, for a channel with constant depth and exponential variation of width.

Sea. The model region, shown in Fig. 1c, with an overall grid size of 20 × 38 is bounded in the north by a line of constant latitude at 60°53′N (at the Shetland Islands) and in the south by the Dover Straits. The average gridsize is 30′ in the east–west direction and 16′ in the north–south direction, corresponding to approximately 29.6 km in both directions. The grid aspect ratio, defined as the ratio of the mean physical length in the $\eta$-direction to that in the $\xi$-direction, varied from 0.29 to 1.8 with an average value of approximately 0.5.

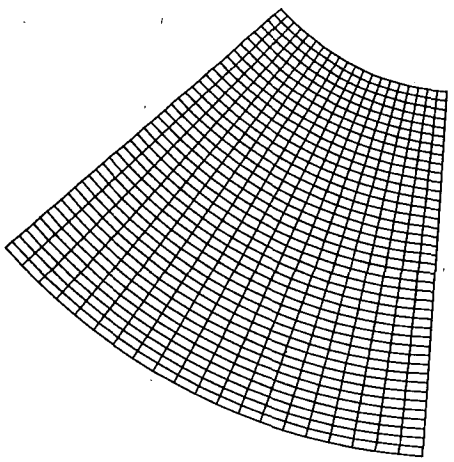

FIG. 3. Grid system employed to define the wedge-shaped section.

The sea elevations (in terms of the $M_2$ range and phase) along the three open boundaries, 1) Shetland Islands to Norwegian coast (along 60°35′N), (2) Dover Straits and (3) Fair Isle region (Shetland to Orkney Islands), were approximated from linear interpolation of data obtained from the Institute of Ocean Sciences, Bidston, England, and the Norwegian Tidal Tables. Depth data to describe the study region were obtained from Norges Sjøkartverk, North Sea Chart 560C (Scale 1:800 000) for the North Sea proper, and from Norges Sjøkartverk, Skagerrak Chart 305D (Scale 1:350 000) for the Skagerrak region.

The model was run at a time step of 74.52 s, resulting in 600 calculations steps per $M_2$ tidal cycle (12.42 h) and a Courant number of 0.8. Simulations were run for five tidal cycles to assure repeatability from cycle to cycle, with typical execution times on a VAX 11/

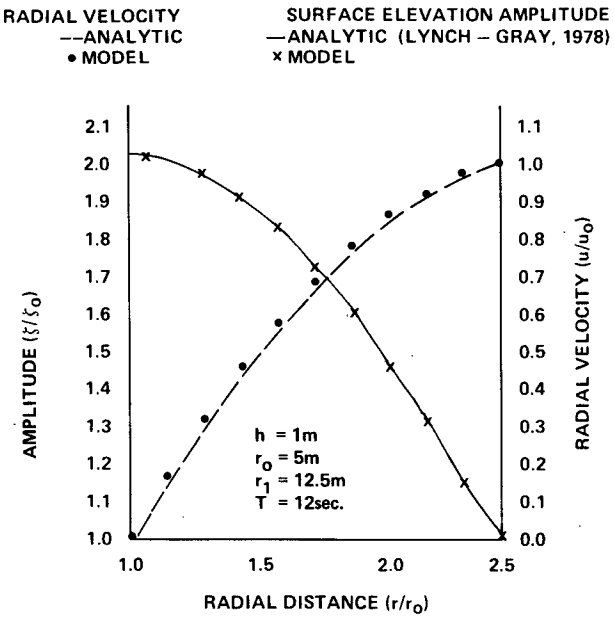


FIG. 4. Comparison of the circulation model predictions for sea-surface elevation and radial velocity with the analytic solution for a flat bottom wedge-shaped domain (Fig. 3). The time corresponds to the maximum in forcing amplitude for the sea surface elevation and to zero forcing amplitude for the radial velocity.

780 of 12 min per cycle. A constant Chezy coefficient of 60 was employed to characterize the bottom frictional losses.

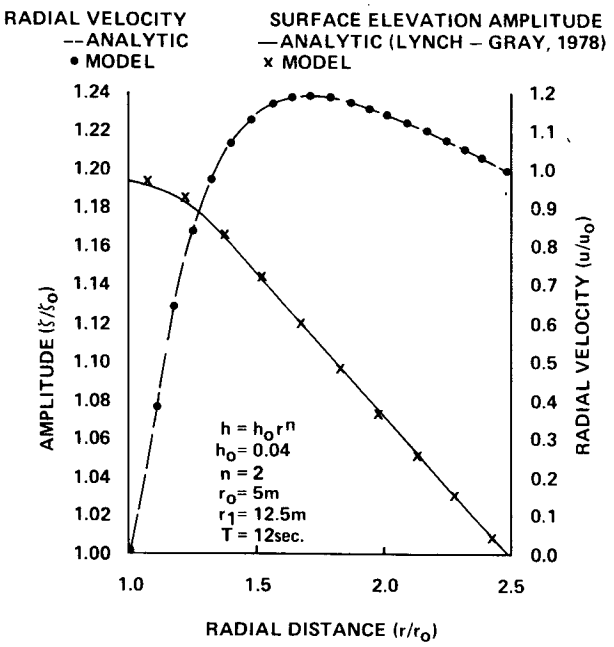


FIG. 5. As in Fig. 4, but for a quadratic sloping bottom wedge-shaped domain (Fig. 3). The time corresponds to the maximum in forcing amplitude for the sea surface elevation and to zero forcing amplitude for the radial velocity.

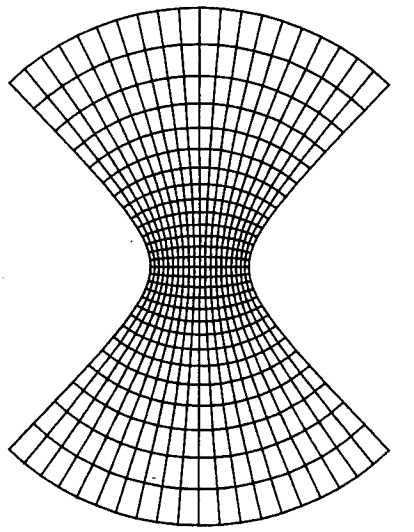

FIG. 6. Grid configuration for model test using an elliptic cylindrical coordinate system. Basin length ~ 90 km, width 17–66 km.

Employing harmonic analysis on the last tidal cycle simulated, the $M_2$ corange–cophase chart was constructed and is shown in Fig. 8. The predicted distributions of amplitude and phase are in good agreement with those obtained from observations by Proudman and Doodson (1924) and the model results of Flather (1976), Davis (1976), Mathisen and Johansen (1983), Marchuk *et al.* (1973), Ronday (1976), Grotkop (1973) and Brettschneider (1966). This can further be appreciated by comparing the present model results with the predictions of Mathisen and Johansen (1983) shown in Fig. 9.

A closer comparison of Fig. 8 to the data and other model predictions indicates that, while the present model accurately predicts the location and character of the amphidromic systems off the southern coast of Norway and in the Dover Straits, the major amphi-

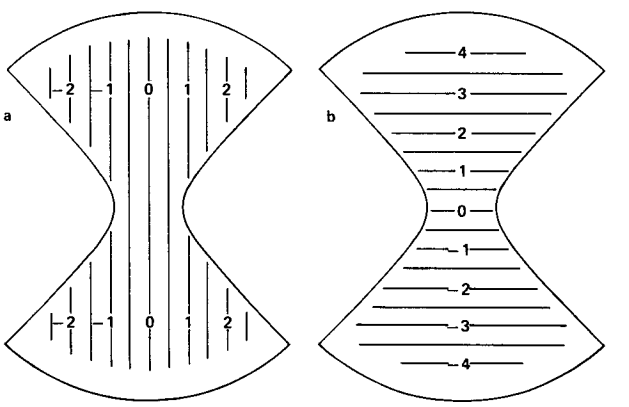


FIG. 7. Steady-state sea surface elevation (cm) in response to (a) 1 dyn $cm^{-2}$ eastward-directed wind stress and to (b) 1 dyn $cm^{-2}$ northward-directed stress.

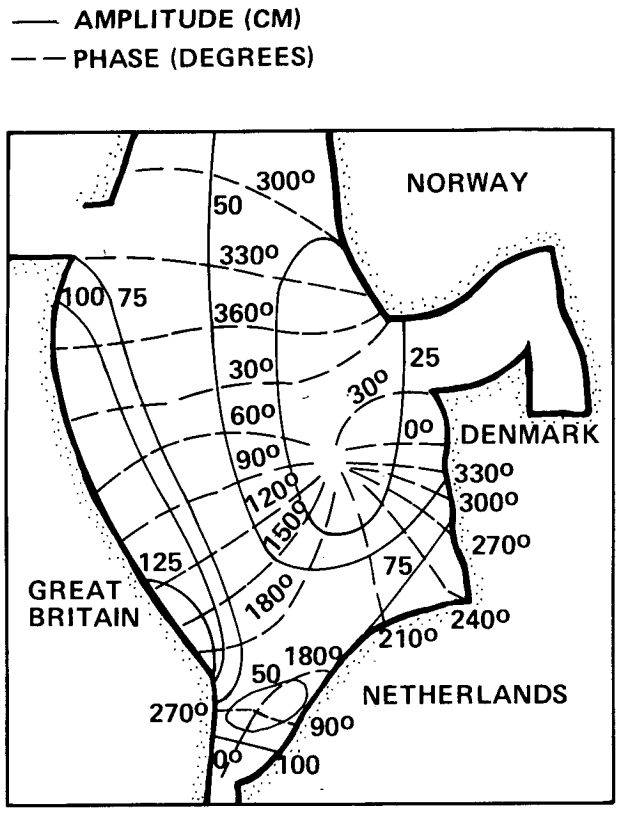


FIG. 8. Model-predicted $M_2$ corange and cophase chart.

dromic point off the Denmark coast, although within the bounds of other modeling studies with similar spatial resolution, is roughly 50 km too far north. The northern displacement of this amphidromic point has resulted in amplitudes larger than observed in the Skagerrak and Kattegat areas. An additional series of simulations with a fourth open boundary prescribed across the entrance to the Skagerrak showed no basic change in the predicted location of this amphidrome. Other simulations varying the horizontal geometry, bathymetry and Chezy factor also showed little impact on the position of this amphidromic region. Based on this series of model studies and other modeling investigations, it is suggested that in order for more accurate predictions to be made a better representation of the study area and a more refined grid structure is necessary.

## 6. Conclusions

A two-dimensional vertically averaged circulation model using boundary-fitted coordinates has been developed for application to estuarine and shelf regions. The use of the boundary-fitted coordinate approach is seen to allow the user extensive control over the design of the computational mesh in order to include both local as well as global adjustments while maintaining a fixed number of computational grids.

Application of the model to a series of simple test cases for which analytic solutions are available for direct comparison has shown the proposed approach to be fully capable of resolving complex geometries while at the same time accurately predicting flow patterns. Preliminary results in applying the model to the North Sea have been encouraging in that the major features of the tidal circulation pattern are predicted.

These simulations have shown, however, that the model predictions are sensitive to the design of the computational mesh. Experience to date, although not definitive in terms of absolute requirements, suggests: 1) that the derivatives of the coordinate points, along lines of constant $\xi$ and $\eta$, defining the model domain, should vary smoothly; 2) that the aspect ratio of the grids be maintained in a range 0.5 to 1.5; and 3) that an attempt be made to have the grids resemble rectangles as closely as possible.

One of the anticipated benefits of the boundary-fitted coordinate circulation model is its improved computational performance (i.e., lower computer costs) in comparison to a simple rectangular grid model for studying circulation in a given area with a specified accuracy. This improvement is achieved by balancing the reduction in computational costs associated with allowing the user to have a more active role in designing a boundary-conforming computational grid, and the increase in computational costs associated with the additional terms introduced into the transformed equations of motion.

Based on the simulations performed here the computational time for the transformed equations is approximately double that for a simple rectangular grid model. Hence if the boundary-fitted circulation model is to be more efficient overall, the reduction in its resolution must at least compensate for this additional computational cost per cell. The overall improvement in model computational performance will therefore be highly problem-dependent.

While the present investigation has established the basic approach, additional work in the following areas is necessary before the proposed methodology can be used for routine application:

1) Computational procedure: Although the multioperational method employed here has been widely tested, allows time steps significantly larger than the Courant limit (while maintaining accurate predictions), and requires less computational resources than a fully implicit method, its advantages are severely compromised in the present application. This is the result of the constantly changing orientation between the $U$ and $V$ velocity vectors and the local grid geometry. In the worst case the computational time step for the present approach is no better than a purely explicit model, but with larger computational costs per time step. It is therefore recommended that the present multioperational difference procedure be replaced by an im-

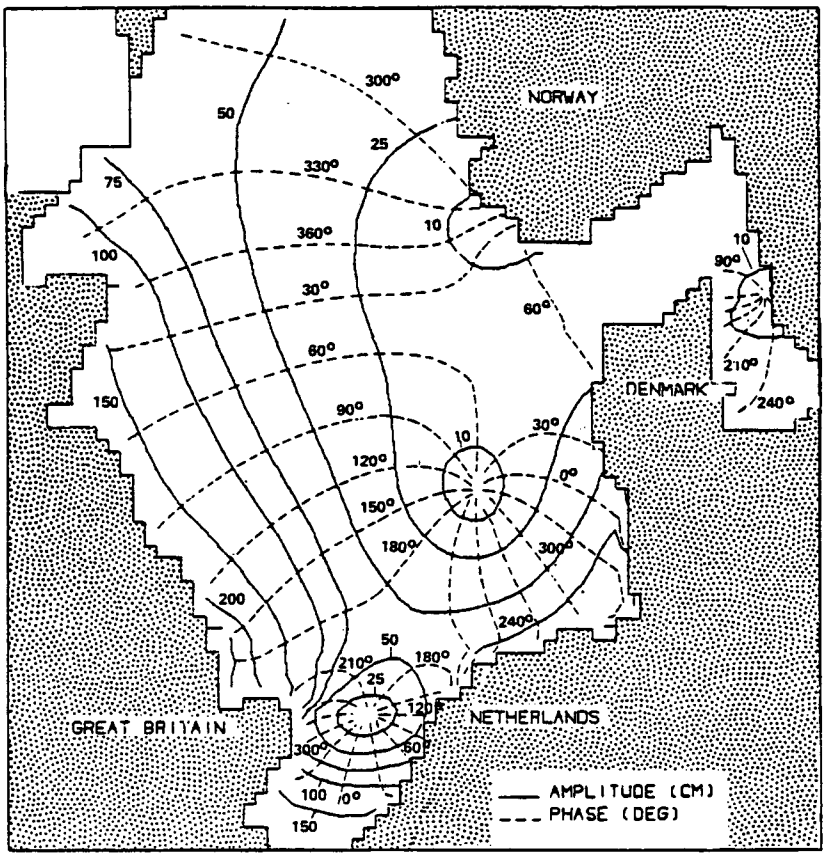


FIG. 9. Mathisen and Johansen (1983) model-predicted $M_2$ corange and cophase chart.

plicit calculation algorithm. This approach should allow a more realistic treatment of the closed boundary conditions (discussed below) and lower computational costs per simulation.

2) Closed boundary treatment: In order to maintain no flux through the closed boundaries under arbitrary grid orientation, and at the same time for the tangential flow to have a simple slip boundary, it was necessary for the velocities at the boundary to vary according to the relationships given by Eq. (13). Unfortunately the use of these specifications implies the need for information at the advanced time level on the opposite velocity field. This information is not available in a standard explicit or multioperational scheme and therefore the quality of the predicted solution decays with time; this is particularly noticeable for long simulations (>5 days). The use of an implicit or even semi-implicit computational procedure should readily address this problem.

3) Dispersion and energy characteristics: The impact of grid deformation on long-wave dispersion and energy characteristics, although treated for simple grid stretching by Lewis *et al.* (1982), has not been documented for the more general case studied here. This is obviously a major deficiency, considering the potential for the continual build up of energy in regions with smaller grid spacing, and the change in phase and group speeds as waves propagate into regions with varying mesh size as noted by Lewis *et al.* A comprehensive test program to document the dispersion characteristics of the numerical scheme is necessary to provide operational guidelines for the use of the boundary-fitted coordinate circulation model.

*Acknowledgments.* This work was completed while the author was on sabbatical leave at the Continental Shelf Institute (IKU), Trondheim, Norway. Funding for the study was provided by a fellowship jointly sponsored by the Royal Norwegian Council for Scientific and Industrial Research and IKU. Computational resources were provided by IKU. The assistance of Dr. Jan-Petter Mathisen in discussing the details of this work and in providing insight into North Sea circulation dynamics is gratefully acknowledged.

## REFERENCES

Arakawa, A., and V. R. Lamb, 1977: Computational design of the basic dynamical process of the UCLA general circulation model. *Methods in Computational Physics,* Vol. 17, Academic Press, 173–265.

ASCE Task Committee on Computational Hydraulics, 1980: Sources of computer programs in hydraulics. *J. Hydraul. Div. Amer. Soc. Civ. Eng.*, **106,** 915–923.

Blumberg, A., and H. J. Herring, 1982: A vertically integrated circulation model using curvilinear coordinates. Prelim. Rep. U.S. Dept. Interior, Contract AA851-CTI-61, 17 pp.

Brettschneider, G., 1966: Hydrodynamical-numerical investigations of the tides in the North Sea. *Proc. Symp. on Mathematical-Hydrodynamical Investigations of Physical Processes in the Sea,* University of Hamburg, 55–59.

Butler, H. L., 1980: Evolution of a numerical model for simulating long-period wave behavior in ocean-estuarine systems. *Estuarine and Wetland Processes,* P. Hamilton and K. MacDonald, Eds., Plenum, 147–182.

Davis, A. M., 1976: A numerical model of the North Sea and its use in choosing locations for the deployment of off-shore tide gauges in the JONSWAP 76 oceanographic experiment. *Dtsch. Hydrogr. Z.,* **29,** 11–24.

Flather, R. A., 1976: A tidal model of the north-west European continental shelf. *Mem. Soc. Roy. Sci. Belg.,* Ser. 6, **10,** 141–164.

Gordon, R., and M. Spaulding, 1974: A bibliography of numerical models for tidal rivers, estuaries and coastal waters. Mar. Tech. Rep. 32, University of Rhode Island, 55 pp.

Grotkop, G., 1973: Finite element analysis of long period water waves. *Comput. Methods Appl. Mech. Eng.,* **2,** 147–157.

Hinwood, J. B., and I. Wallis, 1975: Review of models of tidal waters. *J. Hydraul. Div., Amer. Soc. Civ. Eng.,* **101,** 1404–1421.

Horikawa, K., 1978: *Coastal Engineering—An Introduction to Ocean Engineering.* University of Tokyo Press, 420 pp.

Ippen, A., Ed., 1966: *Estuary and Coastline Hydrodynamics.* McGraw-Hill, 744 pp.

Johnson, B. H., 1980: VAHM—A vertically averaged hydrodynamic model using boundary-fitted coordinates. MP HL-80-3, U.S. Army Engineers Waterways Experiment Station, Vicksburg, MS, 52 pp.

——, 1982: Numerical modeling of estuarine hydrodynamics on a boundary fitted coordinate system. *Numerical Grid Generation,* J. Thompson, Ed., Elsevier, 409–436.

Leenderste, J. J., 1967: Aspects of a computational model for long period water-wave propagation. Rep. RM-5294-PR, Rand Corporation, Santa Monica, CA, 165 pp.

Lewis, J. K., R. E. Whitaker and W. Merrell, 1982: The effects of a stretched-grid coordinate system on long wave dispersion and energy characteristics. *J. Geophys. Res.,* **87,** 4265–4266.

Lynch, D. R., and W. G. Gray, 1978: Analytic solutions for computer flow model testing. *J. Hydraul. Div., Amer. Soc. Civ. Eng.,* **104,** 1409–1428.

Marchuk, G. I., R. G. Gordeev and V. Y. Rivking, 1973: A numerical method for the solution of tidal dynamics equations and the results of its application. *J. Comput. Phys.,* **13,** 15–34.

Mathisen, J. P., 1980: SLIKFORCAST—Neptun C21—A two dimensional numerical model for tidal currents. Ref. P-225/3/80, Continental Shelf Institute, Trondheim, Norway, 48 pp.

——, and Ø. Johansen, 1983: A numerical tidal and storm surge model of the North Sea. *Mar. Geodesy,* **6,** (3–4), 267–291.

Peffley, M. B., and J. J. O'Brien, 1976: A three-dimensional simulation of coastal upwelling off Oregon. *J. Phys. Oceanogr.,* **6,** 164–180.

Pinder, G. F., and W. G. Gray, 1977: *Finite Element Simulation in Surface and Subsurface Hydrology.* Academic Press.

Proudman, J., and A. T. Doodson, 1924: The principal constituent of the tides of the North Sea. *Phil. Trans. Roy. Soc. London,* **A224,** 185–219.

Reid, R. O., A. C. Vastano, R. E. Whitaker and J. J. Wanstrath, 1977: Experiments in storm surge simulation. *The Sea,* Vol. 6, E. D. Goldberg, I. N. McCave, J. J. O'Brien and J. H. Steele, Eds., Wiley, 145–168.

Roache, P., 1972: *Computational Fluid Mechanics.* Hermosa Publishers, 434 pp.

Ronday, F. C., 1976: Modeles de circulation hydrodynamique en Mer du Nord. Ph.D. dissertation, Liège University, Liège, Belgium.

Rottman, K., 1960: *Mathematische Formelsammlung.* Bibliographisches Institut, Mannheim, W. Germany.

Thacker, W. C., 1977: Irregular grid finite-difference techniques: Simulations of oscillations in shallow circular basins. *J. Phys. Oceanogr.* **7,** 284–292.

Thames, F. C., 1975: Numerical solution of the incompressible Navier-Stokes equations about arbitrary two-dimensional bodies. Ph.D. dissertation, Mississippi State University.

——, J. F. Thompson, C. W. Mastin and R. L. Walker, 1977: Numerical solutions for viscous and potential flow about arbitrary two-dimensional bodies using body-fitted coordinate systems. *J. Comput. Phys.,* **24,** 245–273.

Thompson, J. F., F. C. Thames and C. W. Mastin, 1974: Automatic numerical generation of body-fitted curvilinear coordinate systems for fields containing any number of arbitrary two-dimensional bodies. *J. Comput. Phys.,* **15,** 299–317.

——, ——, S. P. Shanks, R. N. Reddy and C. W. Mastin, 1976: Solutions of the Navier-Stokes equations in various flow regimes on fields containing any number of arbitrary bodies using boundary-fitted coordinate systems. *Proc. Fifth Int. Conf. on Numerical Methods in Fluid Dynamics,* Enschede, The Netherlands, *Lecture Notes in Physics,* Vol. 59, Springer-Verlag, 421–427.

——, —— and C. W. Mastin, 1977a: TOMCAT—A code for numerical generation of boundary-fitted curvilinear coordinate systems on fields containing any number of arbitrary two-dimensional bodies. *J. Comput. Phys.,* **24,** 274–302.

——, —— and ——, 1977b: Boundary-fitted curvilinear coordinate system for solution of partial differential equations on fields containing any number of arbitrary two-dimensional bodies. NASA CR-2729.

Waldrop, W. R., and R. C. Farmer, 1974: Three-dimensional computation of buoyant plumes. *J. Geophys. Res.,* **79,** 1269–1276.

——, and F. B. Tatom, 1976: Analysis of the thermal effluent from the Gallatin steam plant during low river flows. Rep. 33-30, Tennessee Valley Authority.

Wanstrath, J. J., 1977: Nearshore numerical storm surge and tidal simulation. TR H-77-17, U.S. Army Engineers Waterways Experiment Station, Vicksburg, MS.